Chemical Engineering Journal 154 (2009) 17–24

Contents lists available at ScienceDirect

Chemical Engineering Journal

journal homepage: www.elsevier.com/locate/cej

Structured reactor with a monolith catalyst fragment for kinetic studies The case of CH_4 partial oxidation on LaNiPt-catalyst

N.N. Sazonova [a], S.N. Pavlova [a], S.A. Pokrovskaya [a,b,*], N.A. Chumakova [a,b], V.A. Sadykov [a,b]

[a] Boreskov Institute of Catalysis, pr. Akademika Lavrentieva 5, Novosibirsk 630090, Russia
[b] Novosibirsk State University, ul. Pirogova 2, Novosibirsk 630090, Russia

ARTICLE INFO

Article history:
Received 14 December 2008
Received in revised form 7 April 2009
Accepted 7 April 2009

Keywords:
Structured reactor
Monolith catalyst
Kinetic studies
Methane
Partial oxidation

ABSTRACT

Analysis of the behavior of a structured reactor of small scale has been fulfilled at millisecond contact times and high temperatures. A single channel fragment of corundum honeycomb substrate with supported LaNiPt active component has been tested in partial oxidation of methane as a model reaction at high gas velocities. Rather high rates of mass transfer are achieved for the conditions under study and the regions are defined with the operation mode where chemical kinetics is rate-controlling. The numerical analysis allows contribution of the direct route of methane oxidation into synthesis gas to be evaluated and some kinetic parameters of main reactions to be estimated.

Suggested design of the lab-scale reactor with separate one-channel structural element of a real monolithic catalyst is shown to be promising for kinetic studies under severe conditions.

1. Introduction

Development of gas-to-liquid technologies and use of fuel cells for the energy generation require elaboration of safe and efficient catalytic processes such as hydrocarbons transformation into the synthesis gas (syngas). The catalytic partial oxidation of methane (POM) could be used for the small-scale and distributed production of syngas in the stationary and mobile fuel processing units [1–3]. This process can also be integrated into the stage combustors of methane for gas turbines wherein methane is partially oxidized in a fuel-rich combustor followed by a fuel-lean combustion [4]. In view of such applications, realization of the process at high gas velocities and contact times less than 0.1 s is a promising route to miniaturize the reactors, which determines the use of monolithic catalysts with a high surface to volume ratio and a low pressure drop [5–7].

Among the challenging problems for developing new catalytic systems and their engineering implementation, the investigation of process kinetics under relevant experimental conditions is one of the main issues due to diffusional limitations and noticeable temperature gradients. Investigating very fast and energy-intensive processes such as catalytic combustion of methane and POM, researchers encounter serious problems related to laboratory fixed-bed reactors wherein the large pressure gradients prevent the use of high flow rates. Under relevant conditions, the external mass transfer limitations and marked temperature gradients can hardly be avoided (see review by Groppi et al. [8]).

The kinetic study of very fast processes realized at high temperatures over monolithic catalysts is rather complicated task which demands elaboration of special structured reactors of small scale operating at high flow velocities with a minimum impact of mass transfer, pressure drop, and temperature gradients along the catalyst length.

Many studies were performed to solve these problems. Previous studies of POM were carried out over the multichannel samples of honeycomb monolithic catalysts [9–12]. For example, the POM kinetic study was performed over the Pt- or Rh-supported monoliths of 9 mm diameter when only four channels were exposed to the gas stream [9,10]. Nickel-supported honeycomb catalysts of 16 mm diameter with 52–64 cells/cm^2 were studied by Lezaun et al. [11]. The experimental and numerical study of the transient behavior of POM was carried out on Rh/α-Al_2O_3 monolith with diameter of 10 mm composed of 24 channels with triangular cross-section [12]. However, only application of different types of microchannel catalytic reactors allows studying the reaction kinetics of fast and strongly exothermic reactions (POM, CH_4 combustion) at short contact times under relevant conditions [1,8,13–18].

A laboratory reactor with flat thin Pt gauze was developed for studying the reactions involved into POM at millisecond contact times [1]. To deal with the problems of kinetic studies at high temperatures and flow rates, a structured annular micro-reactor

* Corresponding author at: Boreskov Institute of Catalysis, pr. Akad. Lavrentieva 5, Novosibirsk 630090, Russia. Tel.: +7 383 3269430; fax: +7 383 3306878.
E-mail address: pokrov@catalysis.ru (S.A. Pokrovskaya).

1385-8947/$ – see front matter © 2009 Elsevier B.V. All rights reserved.
doi:10.1016/j.cej.2009.04.026

Nomenclature

c_i, c_i^s	current concentration of the ith component of the reaction mixture and on the catalyst surface, volume fraction
c_{i0}	concentration of the ith component of the reaction mixture at the channel inlet, volume fraction
D_m	molecular diffusivity of methane (cm^2/s)
d	hydraulic diameter of the channel (cm)
E_j	activation energy of the jth reaction (J/mol)
k_j	constant of the jth reaction rate (s^{-1})
k_{j0}	pre-exponent of the jth reaction rate constant (s^{-1})
$K_{eq,j}$	equilibrium constant of the jth reaction
l	axial coordinate along the channel length (cm)
r_j	rate of the jth reaction ($mol/(cm^3 s)$)
r_i^c	rate of the ith component transformation ($mol/(cm^3 s)$)
R	the universal gas constant (J/(mol K))
S_{sp}	special outer surface of the channel (cm^2/cm^3)
Sh	local Sherwood number
T	temperature (K)
U	superficial gas velocity (cm/s)
z^*	dimensionless axial coordinate

Greek letter

β	local mass transfer coefficient at the channel wall (cm/s)

Subscripts

i	number of the compound of the reaction mixture (i = 1 corresponds to methane; 2, oxygen; 3, carbon oxide; 4, hydrogen; 5, carbon dioxide; and 6, water)
j	number of the reaction, j = 1,2,3,4
∞	asymptotic value at the infinity

consisting of a ceramic tube coated with a small amount of a catalyst was developed [13]. The characterization of the behavior of annular reactor for kinetic measurements was done in [8,14] addressing a deeper understanding of the reactor potentialities. Detailed theoretical and experimental studies of the annular reactor performance demonstrated its adequacy for kinetic investigation of ultra-fast catalytic reactions such as CH_4 partial oxidation and methane or CO combustion [15–17].

Recently, we have studied POM at millisecond contact times on the catalysts based on mixed $MeCeZrO_x$ solid solution promoted by Pt and/or Ni and supported on separate structured elements of the monolithic substrates of different types such as the fragments of ceramic honeycomb monolith with one triangular channel, the gauze rolls, and the wire spiral placed into a thin quartz tube reactor [18,19].

This work aims at detailed analysis of the performance features of a structured reactor with a monolithic $LaNiPt/CeZrO_x$-catalyst based on a honeycomb α-Al_2O_3 support with triangular channels. The results of the first stage of experimental and numerical studies of the reaction of methane partial oxidation in the tube reactor with a separate catalytic fragment with one channel at 4–15 ms contact times are reported below. The studies are focused on the resources of lab-scale reactor of suggested design for kinetic measurements. Mass transfer rates are defined and the reactor potentialities for kinetic studies of fast and highly exothermic reactions are shown.

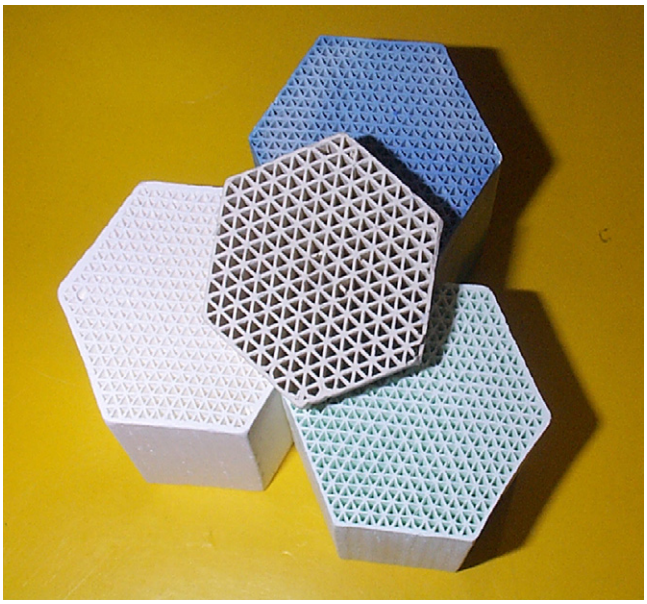

Fig. 1. Samples of monolithic catalyst based on a honeycomb α-Al_2O_3 support with triangular channels.

2. Experimental

2.1. Catalyst preparation

As supports, separate triangular fragments of α-Al_2O_3 monolith (the specific surface area of 3 m^2/g) sintered at 1300 °C, with the wall thickness of 0.2–0.3 mm, the side of the inside triangular channel of 2.3–2.5 mm, and the length of 10–20 mm were used. $Zr_{0.8}Ce_{0.2}O_2$ (10 wt%) and $LaNi_{0.9}Pt_{0.1}O_x$ (7 wt%) were supported by the incipient wetness impregnation first with the mixed solution of $Ce(NO_3)_3$ and $ZrOCl_2$ and then, with the mixed solution of La and Ni nitrates and H_2PtCl_6. After each impregnation, the samples were dried and calcined at 900 °C in air. According to the previous study [20], the $LaNiO_3$ perovskite phase of the hexagonal structure and $Zr_{0.8}Ce_{0.2}O_2$ solid solution are present in the catalysts.

The shape and structure of the catalyst fragments prepared in such a way correspond completely to those for the real catalytic monolith shown in Fig. 1.

2.2. Reactor unit

The testing of the catalysts was carried out in a quartz tube reactor of 4–6 mm inner diameter and 40 cm length. Schematic drawing of the reactor unit is given in Fig. 2. The catalyst fragment with one channel was placed into the quartz tube reactor, and the space between the catalyst and the reactor wall was sealed up with α-Al_2O_3 fiber, so that the reaction mixture went only through the inner channel volume. The quartz tube was placed in the two-zone 30 cm long electric oven. The first part of the oven heated up the gas reactant mixture supplied to the catalyst. The coiled fechraloy gauze was installed in the reactor at 2 cm distance from the channel inlet to provide more effective preheating of the feed. Another part of the oven kept a prescribed reaction temperature. There were two thermocouples to determine the temperature of ovens, and two more thermocouples at the front and rear edges of the channel were used to measure the catalyst temperature. To decrease the heat losses, thin (0.1–0.2 mm diameter) chromel–alumel thermocouples were used. The temperatures of the catalyst and the oven were controlled and continuously monitored by an "ADAM" unit.

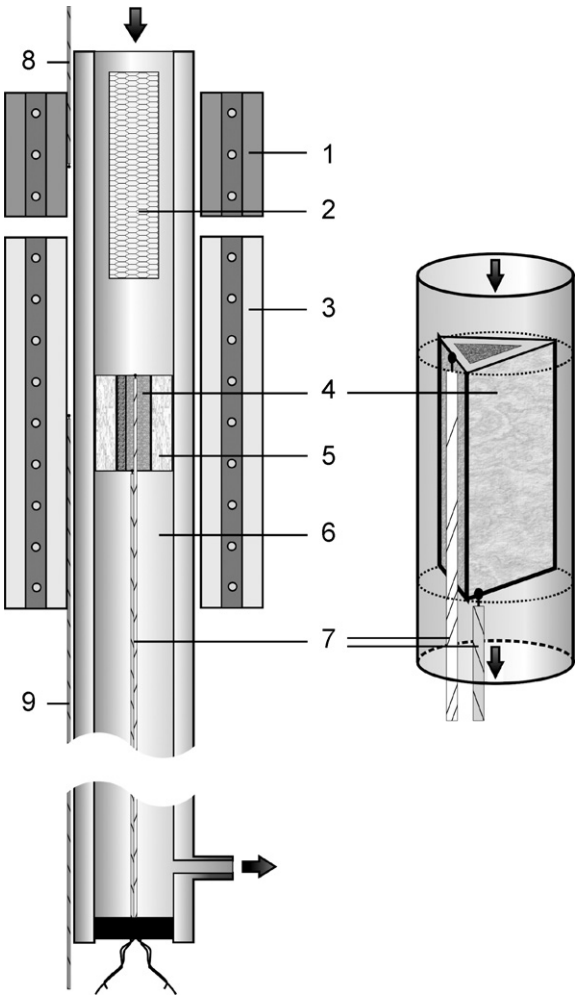

Fig. 2. Scheme of reactor equipments: 1 – oven for the gas flow heating; 2 – coiled gauze; 3 – oven for the catalytic reactor heating; 4 – catalyst fragment with one channel; 5 – alumina fiber; 6 – quartz tube, 7–9 – thermocouples.

Three lines equipped with the mass-flow meters were used to feed CH_4, O_2, and N_2. The gases were mixed upstream from the reaction zone in a special mixer.

The reagents and reaction products were analyzed by GC (a "TSVET-500" chromatograph) and/or a "TEST-201" gas analyzer with the data acquisition and processing with a computer. In the gas analyzer, IR absorbance sensors were used for measurements of CH_4, CO, and CO_2, while O_2 and H_2 concentrations were determined by the electrochemical and polarographic sensors, respectively. In the chromatograph, NaX Molecular Sieve column and thermoconductivity detector were used for determination of the H_2 and O_2 concentrations, while CO, CO_2, and CH_4 were separated on Chromosorb-102 column. The mean values of measured concentrations were used to calculate the methane conversion, the selectivity of the products, and the C-balance.

All data presented below correspond to the stationary state of the catalyst reached in 1 h after setting new operation conditions. The data of GC analysis and gas analyzer were in a good agreement. The concentrations were determined with error below 5%.

3. Experimental results

3.1. POM reaction

The temperature of the catalyst was varied in the range of 600–850 °C. All experiments were carried out at the atmospheric pressure. The catalysts were pretreated at 700 °C for 1 h in the oxygen flow and then for 30 min in the flow of 20 vol.% H_2 in He. At the reaction temperature, the reactant mixture comprised of 1.5–7 vol.% CH_4 and 0.7–4 vol.% O_2 in N_2 was fed into the reactor with the flow rate in the range of 5–30 l/h corresponding to superficial velocity of 70–300 cm/s (STP) and 4–15 ms contact time. Blank experiments confirmed that the homogeneous reactions did not proceed for the conditions under study.

A set of experimental runs with variation of the contact time, the temperature, and the feed composition were carried out to study

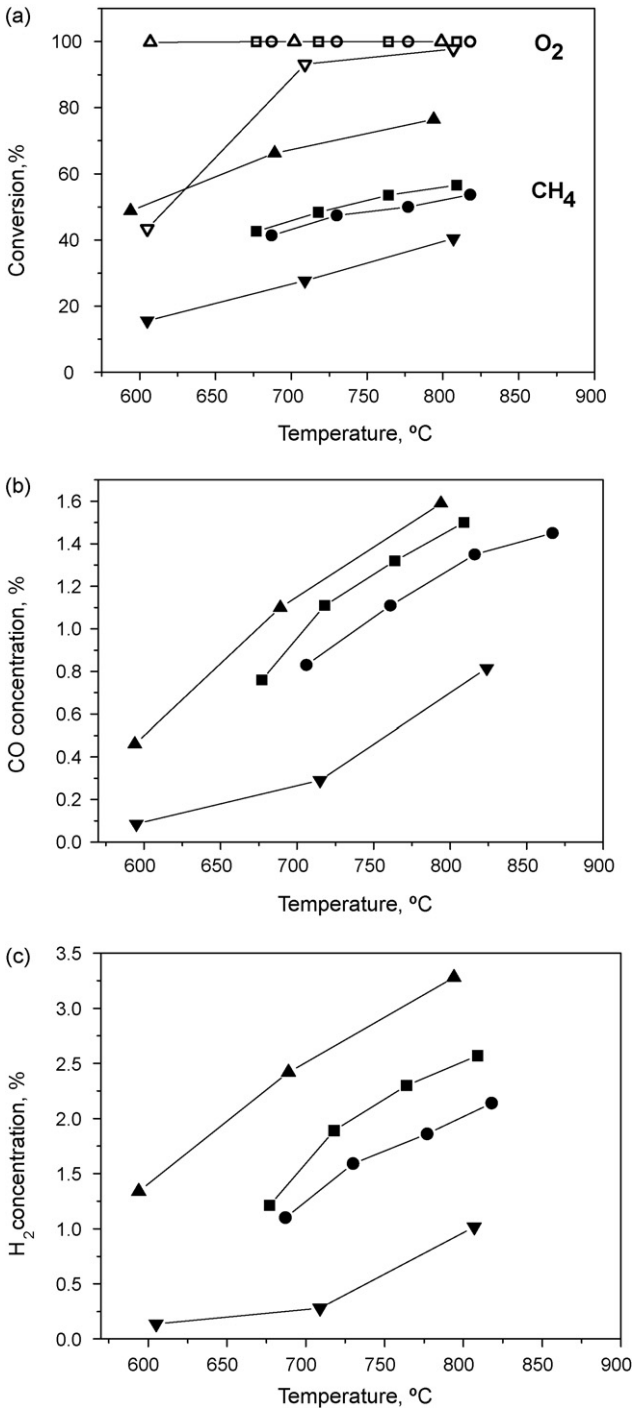

Fig. 3. Temperature dependences of O_2 and CH_4 conversion (a) and product concentrations (b, c), 3.5% CH_4 + 1.75% O_2 in the feed, contact time of 4.7 ms (▽, ▼), 6 ms (○, ●), 8 ms (□, ■) and 15 ms (△, ▲).

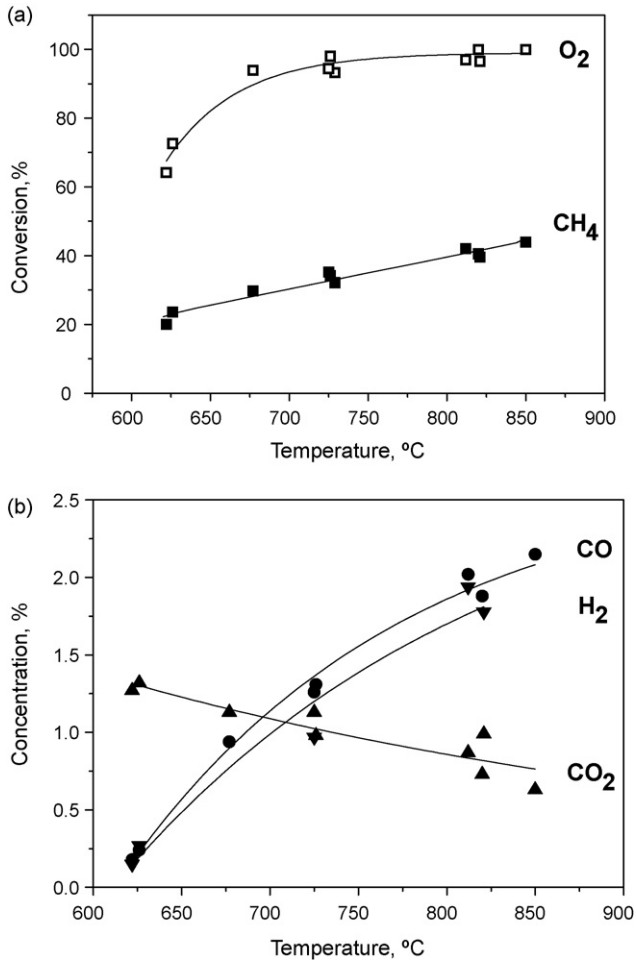

Fig. 4. Temperature dependences of O_2 and CH_4 conversion (a) and product concentrations (b) for the contact time of 4.7 ms, 10 mm channel, 7% CH_4 + 3.5% O_2 in the feed. Symbols – (a) O_2 (□), CH_4 (■); (b) CO (●), H_2 (▼), CO_2 (▲).

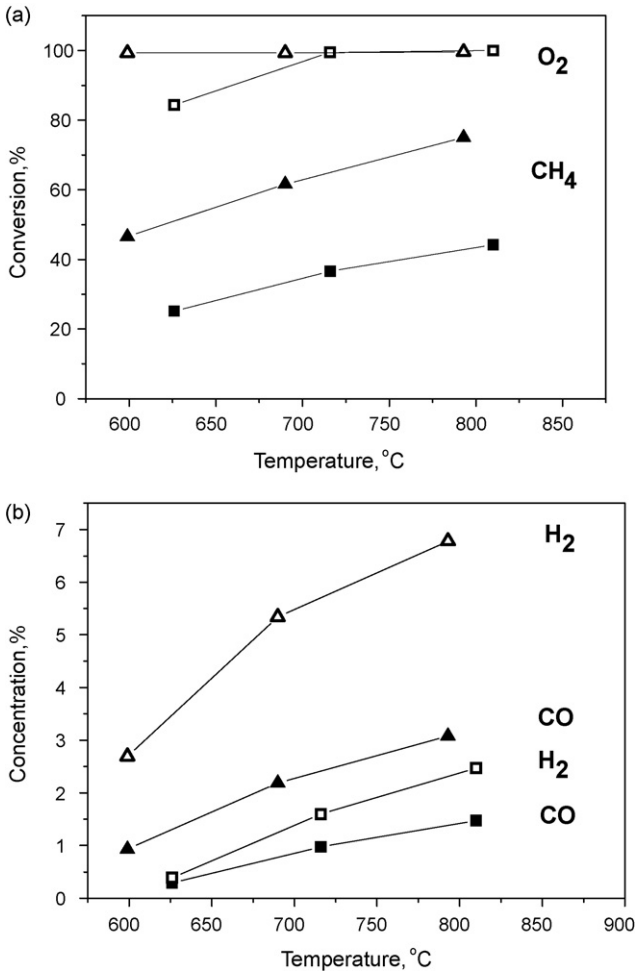

Fig. 5. Temperature dependences of O_2 and CH_4 conversion (a) and product concentrations (b), 10 mm channel, 7% CH_4 + 3.5% O_2 in the feed, contact time of 8 ms (□, ■) and 15 ms (△, ▲).

the dependence of the reagent conversion and product (H_2, CO, CO_2) selectivity on the operation conditions. The main experimental regularities were found to be similar to those earlier obtained for LaNi-catalyst samples [18].

Figs. 3–5 show typical temperature dependences of reagent conversions and product concentrations versus exit temperature measured at the rear part of the channel.

For all studied conditions, a rise of temperature and/or contact time increases methane and oxygen conversion and syngas (CO and H_2) selectivity. At higher contact times and temperatures, when the oxygen consumption is complete (Figs. 3 and 5), this trend implies operation of the indirect pathway of methane oxidation. The rise of CH_4 conversion and CO selectivity indicates that first CH_4 combustion in the inlet part of the channel is followed by steam and dry reforming reactions of remaining methane in the oxygen-free reactor zone, so CO and H_2 become the main products at temperatures above 750 °C. The product distribution confirms the syngas to be generated via the consecutive route.

At temperatures below 750 °C and lower contact times, the oxygen conversion is incomplete. Figs. 3 and 4 show that syngas is formed in the presence of gaseous O_2. This implies operation of the direct route of methane transformation to syngas under these conditions, since in the presence of oxygen the reactions of methane steam and dry reforming are expected to be suppressed.

For all experiments, the temperature gradients along the fragment length are observed, the inlet temperature being higher than the outlet one. The temperature difference between the inlet and the outlet is in the range of 7–35 °C. The temperature gradient rises with the increase of temperature and/or inlet CH_4 concentration that points to the contribution of the exothermic oxidation of methane in the initial part of the channel. The decrease of the contact time lowers the contribution of the endothermic reforming reactions along the catalyst fragment.

3.2. Steam and dry reforming reactions

To estimate the role of secondary reactions, the dry and steam reforming were studied for the same separate fragment of LaNiPt/corundum catalyst with the inlet reactant mixture containing $CH_4 + CO_2$ and $CH_4 + H_2O$ in nitrogen. The experimental data were obtained for the same temperatures and contact times as for POM. Some typical temperature dependences of methane conversion for the dry and steam reforming reactions are given in Fig. 6. For all conditions, the rates of these reactions increase with the temperature agreeing with conclusion on their contribution to POM at high temperatures.

3.3. Activity comparison

The first-order rate constants with respect to the concentration of methane were evaluated from the independent data of POM, steam and dry reforming reactions described above in Sections 3.1 and 3.2 (Figs. 3–6). The typical values of constants are given in

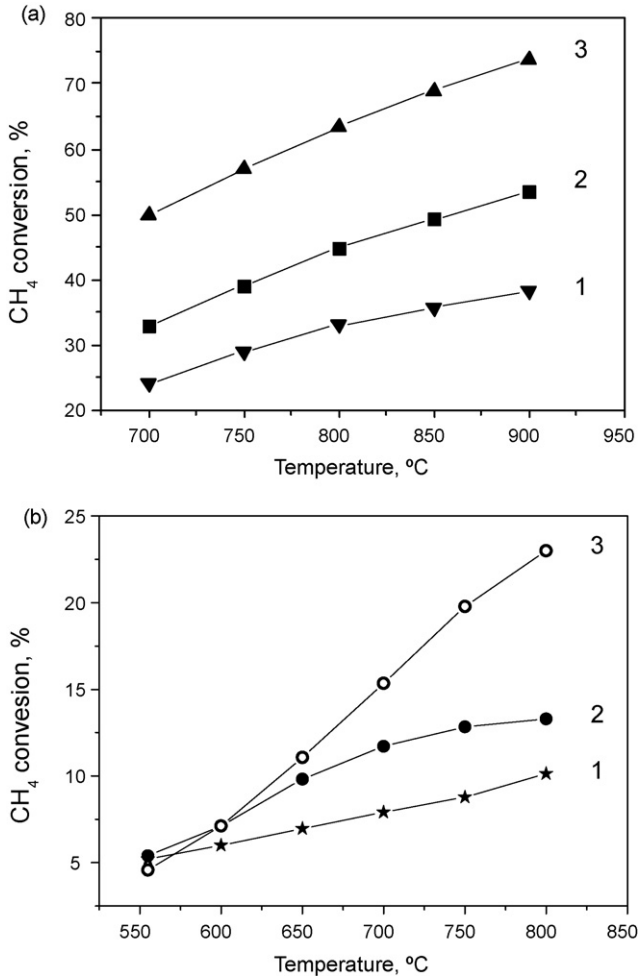

Fig. 6. Temperature effect on CH_4 conversion for dry (a) and steam (b) reforming reactions: (a) 7% CH_4 + 7% CO_2 in the feed, 20 mm channel, contact times of 4.7 ms (1), 8 ms (2), 15 ms (3); (b) 10 mm channel, 6 ms contact time, 7% CH_4 in the feed, CH_4:H_2O ratio in the feed is 1:1 (1), 1:1.8 (2), 1:3 (3).

Table 1. The catalyst activity for POM is evaluated through the concentration of methane because from the data presented in Section 3.1 it follows that methane could convert in POM through the four reactions – direct oxidation to CO and H_2 as well as deep oxidation followed by steam and dry reforming reactions. As follows from Table 1, the values of dry and steam reforming rate constants are comparable with those of partial methane oxidation, which implies that a significant part of methane is converted into syngas via the indirect route including the combustion of methane followed by the subsequent steam and dry reforming of remaining methane.

Table 1
Catalyst activity.

Initial components	CH_4%, input	O-containing comp.%, input	T_{out} (°C)	τ (ms)	X_{CH_4} (%)	k (s^{-1})
$CH_4 + O_2$	3.2	1.5	605	4.7	15.6	71
	6.7	3.0	633	4.7	17.7	84
	3.11	1.6	696	8	40.0	139
	3.45	1.7	711	4.7	28.4	157
	3.1	3.0	799	8	53	227
	3.58	1.73	806	6	38.3	194
$CH_4 + CO_2$	6.49	6.96	575	8	15.1	33.9
	7	6.96	675	8	29.4	92.7
$CH_4 + H_2O$	7	12.6	600	5.7	7	26
	7	12.6	700	5.7	11.7	48

These estimations are used further to clarify the mass transfer influence on the catalyst performance and estimate the initial fitting for the data processing.

4. Numerical analysis

4.1. Mathematical model

Mathematical description of the catalytic reaction behavior in the structured reactor under study is based upon the following assumptions: the axial diffusion is not significant; the intraporous diffusion resistance is negligible; the reaction occurs at conditions close to isothermal ones.

To estimate possible axial diffusion in the channel, the Peclet number is calculated for the conditions under study. For the channel length of 10 mm, the Peclet number is higher than the limit value of 50 above which the axial dispersion in the gas phase may be neglected [21]. The Thiele criterion estimated with the values of catalyst activity in POM (Table 1) is lower than 0.5, so the intraporous diffusion resistance affects the reaction rate insignificantly [22].

Analysis of the temperature gradients along the fragment length for the experimental points given above shows that, for all data with inlet CH_4 concentration below 3.5 vol.%, the measured temperature difference between the fragment inlet and outlet does not exceed 15 °C. For higher inlet CH_4 concentrations, the temperature gradients increase and achieve the values up to 35 °C for experiments carried out at 750–800 °C with methane conversion higher than 85–90%. The experimental points with the temperature gradients of at most 20 °C are selected for further data processing. Though the isothermal model is used below for kinetic analysis, the mean error brought of this assumption does not exceed 10%. The constant volume reaction can be assumed because the experiments were carried out with inlet methane concentration of at most 7 vol.% and methane conversion up to 60%, and hence the mean deviation of the gas volume was not higher than 3% in this case.

The simple one-dimensional model includes the mass balances for the reacting species in the gas-phase and on the channel wall:

$$\begin{aligned} &U\frac{dc_i}{dl} = -S_{sp}\beta(l)(c_i - c_i^s),\\ &S_{sp}\beta(l)(c_i - c_i^s) = r_i^c(c_1^s, \ldots, c_6^s),\\ &l = 0: \quad c_i = c_{i0}, \end{aligned} \tag{1}$$

where the indices correspond to methane (i = 1), oxygen (2), carbon oxide (3), hydrogen (4), carbon dioxide (5), and water (6).

The mass transfer coefficients between the gaseous flow and the catalytic wall are determined on the basis of approach for the local Sherwood number in honeycomb monolith matrices [23]:

$$Sh = Sh_\infty + 6.874 \times (1000z^*)^{-0.545}\ \exp(-57.2z^*), \quad \text{where } z^* = \frac{lD_m}{Ud^2}.$$

4.2. Mass transfer rates

The axial profiles of the Sherwood number and the mass transfer coefficients are defined for the ranges of temperatures and gas flow rates given above. The evaluations are obtained for methane (the main reactant in the gas mixture) and also valid for other components due to close values of the molecular diffusivities. Fig. 7 shows the axial profiles of the Sherwood number for temperatures of 600, 700, and 800 °C at the flow rate of 18 l/h and for different feed rates at 700 °C. More than three-fold decrease of the Sherwood number value along the catalyst length is observed. In Fig. 8, similar dependences are given for the inter-phase mass transfer coefficients referred to the channel volume to compare these values

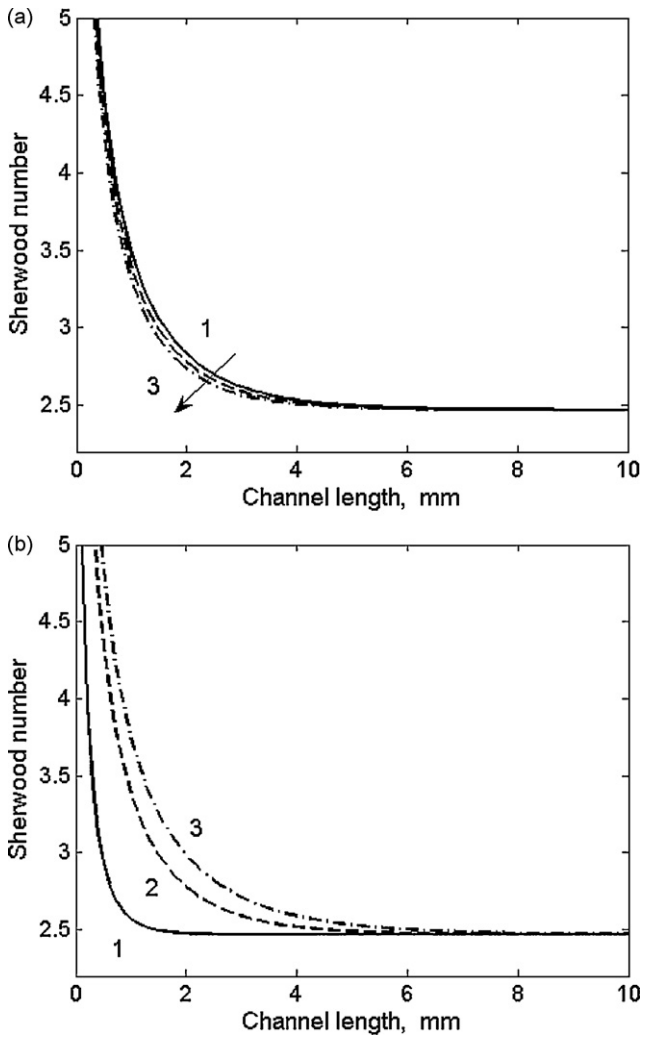

Fig. 7. Sherwood number along the fragment channel (calculated for methane): (a) gas flow rate of 18 l/h, temperature of 600 °C (1), 700 °C (2), 800 °C (3); (b) temperature of 700 °C, gas flow rate of 5.6 l/h (1), 18 l/h (2), 24 l/h (3).

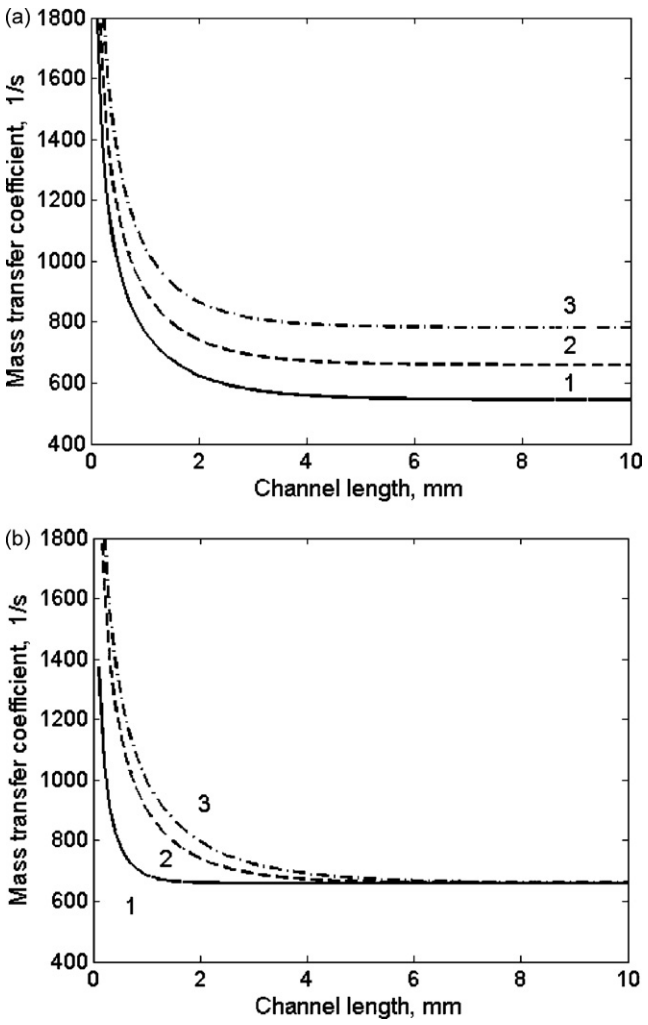

Fig. 8. Inter-phase mass transfer coefficient β along the fragment channel (calculated for methane): (a) gas flow rate of 18 l/h, temperature of 600 °C (1), 700 °C (2), 800 °C (3); (b) temperature of 700 °C, gas flow rate of 5.6 l/h (1), 18 l/h (2), 24 l/h (3).

with the catalyst activity. It is seen that under studied conditions the inter-phase mass transfer stabilizes in the middle of the whole channel length. The most intensive changing and mixing of the gas stream appear near the channel inlet, which causes the highest local rates of the inter-phase exchange process at the distance up to 2 mm. By analogy to the Sherwood number, the local mass transfer coefficients differ by more than three times along the channel length.

Fig. 9 presents the regions of mass transfer intensity at different operation conditions. These regions with different mass transfer rates are plotted for three points along the channel length: 0.5 mm, where the rate is rather high, at the axial point of 2 mm, and at the channel end (10 mm). Even at the channel end, where the Sherwood number is almost equal to the asymptotic value, the mass transfer coefficients reach the values of 700–800 1/s at 750–800 °C. At the distance of 2 mm from the inlet, such values are attained for high space velocities at lower temperatures. At last, at the inlet part of the channel, the mass transfer rates have the same values for temperatures of 400–500 °C and even amount up to 1000 l/s at 500–600 °C.

The comparison of mass transfer coefficients determined (Fig. 9) and the values of catalyst activity (Table 1) shows that, in this structured reactor, the mass transfer rate exceeds significantly the rates of POM as well as dry and steam reforming reactions and allows to select the experimental data, where the reaction occurs in the operation mode chemically controlled.

Thus, the experimental points with minimal influence of the mass transfer as well as minimal temperature gradients are taken

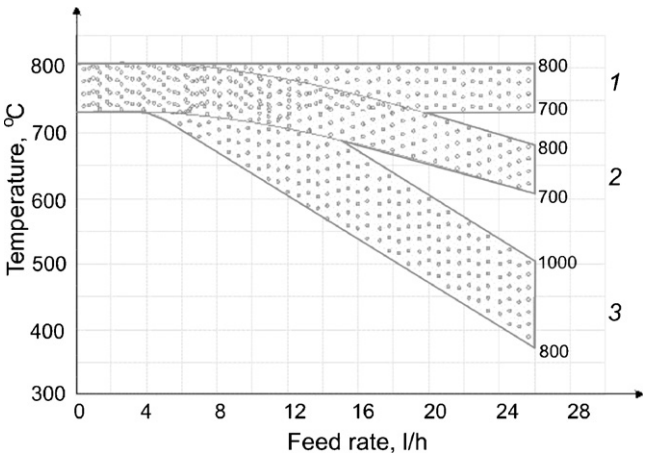

Fig. 9. The regions of mass transfer coefficients β at different points l along the channel length: 1 – channel end, l = 10 mm, β = 700–800 s^{-1}; 2 – l = 2 mm, the same values of β; 3 – beginning of the channel, l = 0.5 mm, β = 800–1000 s^{-1}.

for further data processing. In what follows, the mathematical model for the ideal plug flow reactor is applied.

4.3. Data processing

The chosen data are processed to determine quantitatively the contribution of direct route of methane selective oxidation into syngas generation and to estimate kinetic parameters of the main reactions.

As it has been discussed in Section 3.1, according to the experimental data obtained, the direct and indirect routes of syngas formation in POM should be considered for catalysts with LaNiPt/CeZrO$_x$ active component [19]:

Direct route:

1. $CH_4 + 0.5O_2 \rightarrow CO + 2H_2$

Consecutive route:

2. $CH_4 + 2O_2 \rightarrow CO_2 + 2H_2O$

3. $CH_4 + H_2O \leftrightarrow CO + 3H_2$

4. $CH_4 + CO_2 \leftrightarrow 2CO + 2H_2$

The following kinetic expressions are used:

$$r_1 = k_1 c_{CH_4} c_{O_2}^{0.5}, \quad r_2 = k_2 c_{CH_4} c_{O_2},$$

$$r_3 = k_3 c_{CH_4} c_{H_2O} \left(1 - \frac{c_{CO} c_{H_2}^3}{c_{CH_4} c_{H_2O}} \frac{1}{K_{eq3}}\right),$$

$$r_4 = k_4 c_{CH_4} c_{CO_2} \left(1 - \frac{c_{CO}^2 c_{H_2}^2}{c_{CH_4} c_{CO_2}} \frac{1}{K_{eq4}}\right),$$

where $k_j = k_{j0} \exp(-E_j/RT)$, $j = 1,2,3,4$.

At the first stage of data processing, only the indirect route with three main reactions (2), (3) and (4) (Scheme 1) is analyzed, and, at the second stage, the reaction (1) of direct oxidation is added (Scheme 2).

Fig. 10 shows an example of fitting, and the model parameters are given in Table 2. The experimental and calculated points are in a good agreement for both schemes. The experimental data processing allows the kinetic characteristics of deep methane oxidation, steam and dry reforming as well as the contribution of the direct route of POM to be evaluated (see Table 2). These preliminary results show that the rate of direct oxidation of methane into syngas is not high.

Since the fitting of experimental data within both Schemes 1 and 2 is equally good, this implies that some correlation of kinetic parameters exists for Scheme 2. This means that it is necessary to enlarge the experimental basis for kinetic analysis and to extend the range of operation conditions, especially in the presence of unreacted O_2 at temperatures below 700 °C and contact times not exceeding 5 ms. Processing of enlarged set of experimental data could allow to determine the contribution of direct oxidation route more precisely and obtain the independent kinetic parameters.

Note that the transient kinetic experiments (attainment of the catalyst steady state after jump of the inlet concentrations of reactants) could be informative for the purpose, and this reactor allows carrying out these experiments as well.

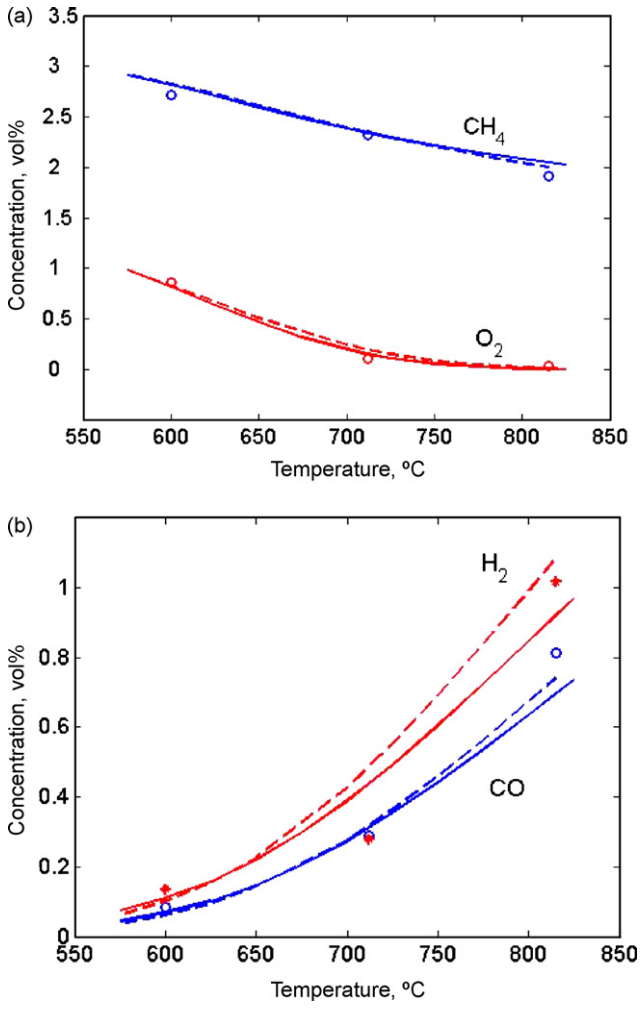

Fig. 10. Experimental (symbols) and calculated (lines) effect of temperature on the reagent and product concentrations, 3.5% CH_4 + 1.75% O_2 in the feed, temperature of 700 °C, contact time of 4.7 ms. Dash lines – Scheme 1, solid lines – Scheme 2.

Table 2
The kinetic parameters.

Kinetic parameters	Scheme 1: consecutive route	Scheme 2: direct and consecutive routes
k_{10} (ms^{-1})	–	40
k_{20} (ms^{-1})	2.9×10^5	7×10^5
k_{30} (ms^{-1})	220	120
k_{40} (ms^{-1})	1.4×10^4	1.35×10^4
E_1 (kJ/mol)	–	59
E_2 (kJ/mol)	86	92
E_3 (kJ/mol)	46	46
E_4 (kJ/mol)	70	70

5. Conclusion

The study of the behavior of the small-scale structured reactor at millisecond contact times and high temperatures is fulfilled in order to verify the reactor potentialities for kinetic measurements. The catalytic tests for partial oxidation of methane are performed in the quartz tube with the one-channel fragment of a monolithic honeycomb LaNiPt/CeZrO$_x$/α-Al_2O_3 catalyst. The shape and structure of the fragment correspond completely to the properties of the real monolithic catalyst.

The influence of operation conditions on the conversion of reagents and the selectivity of products is determined. At higher

temperatures and/or longer contact times, syngas is generated via the consecutive route, including methane combustion followed by dry and steam reforming reactions. This conclusion is supported by estimation of the activity of the same one-channel catalyst fragment in dry and steam reforming reactions. At shorter contact times and lower temperatures, when oxygen conversion is incomplete, syngas can form through the direct route of methane selective oxidation as well.

The rates of the inter-phase exchange between the gaseous flow and the catalyst channel wall are defined and the mass transfer influence on the reaction rate is analyzed. The performance of catalytic tests at high gas velocities allows rather high mass transfer rates in the structured reactor to be provided. To compare the catalyst activity and the mass transfer rates evaluated under all studied conditions in a channel of monolith, the regions are defined, wherein the reaction occurs in chemical or chemical-diffusion controlled operation mode. For further data processing, the experimental points are selected with minimum influence of the mass transfer and axial temperature gradients.

Kinetic characteristics of deep methane oxidation as well as steam and dry reforming are evaluated by the data processing. The contribution of the direct route of partial oxidation of methane into syngas is estimated as well as the region of operation conditions is determined for the further series of experimental runs to define this contribution more precisely and to obtain independent kinetic parameters.

Thus, the studies performed show that developed design of the small-scale reactor with the separate structured element of a real catalyst is promising for the kinetic studies under severe conditions. This reactor can be used also as an effective tool to predict the characteristics of a catalytic process for real industrial conditions.

Acknowledgements

This work was supported by Internal Project of Boreskov Institute of Catalysis and by RFBR-CNRS 05-03-34761 Project. The authors are grateful to E.L. Gubanova, R.V. Bunina, and A.S. Bobin for providing some experimental data.

References

[1] M.-F. Reyniers, C.R.H. Smet, P.G. Menon, G.B. Marin, Catalytic partial oxidation, Part I, CATTECH 6 (2002) 140–149.
[2] C. Song, Fuel processing for low-temperature and high-temperature fuel cells: challenges, and opportunities for sustainable development in the 21st century, Catal. Today 17 (2002) 17–49.
[3] B.C. Enger, R. Lodeng, A. Holmen, A review of catalytic partial oxidation of methane to synthesis gas with emphasis on reaction mechanisms over transition metal catalysts, Appl. Catal. A: Gen. 346 (2008) 1–27.
[4] M. Lyubovsky, L.L. Smith, M. Castaldi, H. Carim, B. Nentwick, S. Etemad, R. LaPierre, W.C. Pfefferle, Catalytic combustion over platinum group catalysts: fuel-lean versus fuel-rich operation, Catal. Today 83 (2003) 71–84.
[5] D.A. Hickman, L.D. Schmidt, Synthesis gas formation by direct oxidation of methane over Pt monoliths, J. Catal. 138 (1992) 267–282.
[6] T. Giroux, S. Hwang, Y. Liu, W. Ruettinger, L. Shore, Monolithic structures as alternatives to particulate catalysts for the reforming of hydrocarbons for hydrogen generation, Appl. Catal. B: Environ. 55 (2005) 185–200.
[7] J. Chen, H. Yang, N. Wang, Z. Ring, T. Dabros, Mathematical modeling of monolith catalysts and reactors for gas phase reactions, Appl. Catal. A: Gen. 345 (2008) 1–11.
[8] G. Groppi, W. Ibashi, E. Tronconi, P. Forzatti, Structured reactors for kinetic measurements in catalytic combustion, Chem. Eng. J. 82 (2001) 57–71.
[9] K. Heitnes, S. Lindberg, O.A. Rokstad, A. Holmen, Catalytic partial oxidation of methane to synthesis gas using monolithic reactors, Catal. Today 21 (1994) 471–480.
[10] K.H. Hofstad, B. Andersson, A. Holmgren, O.A. Rokstad, A. Holmen, Partial oxidation of methane to synthesis gas—experimental and modeling studies, Stud. Surf. Sci. Catal. 107 (1997) 415–420.
[11] J. Lezaun, J.P. Gomez, M.D. Blanco, I. Cabrera, M.A. Pena, J.L.G. Fierro, Characterization of Ni-honeycomb catalysts for high pressure methane oxidation, Stud. Surf. Sci. Catal. 119 (1998) 729–734.
[12] R. Schwiedernoch, S. Tischer, C. Correa, O. Deutschmann, Experimental and numerical study of the transient behavior of partial oxidation of methane in a catalytic monolith, Chem. Eng. Sci. 58 (2003) 633–642.
[13] J.G. McCarty, Kinetics of PdO combustion catalysis, Catal. Today 26 (1995) 283–293.
[14] A. Beretta, P. Baiardi, D. Prina, P. Forzatti, Analysis of a catalytic annular reactor for very short contact times, Chem. Eng. Sci. 54 (1999) 765–773.
[15] I. Tavazzi, A. Beretta, E. Tronconi, P. Forzatti, An investigation of methane partial oxidation kinetics over Rh-supported catalysts, Stud. Surf. Sci. Catal. 147 (2004) 163–168.
[16] M. Maestri, A. Beretta, G. Groppi, E. Tronconi, P. Forzatti, Comparison among structured and packed-bed reactors for the catalytic partial oxidation of CH_4 at short contact times, Catal. Today 105 (2005) 709–717.
[17] A. Donazzi, A. Beretta, G. Groppi, P. Forzatti, Catalytic partial oxidation of methane over a 4% Rh/α-Al_2O_3 catalyst. Part I. Kinetic study in annular reactor, J. Catal. 255 (2008) 241–258.
[18] S. Pavlova, N. Sazonova, V. Sadykov, S. Pokrovskaya, V. Kuzmin, G. Alikina, A. Lukashevich, E. Gubanova, Partial oxidation of methane to synthesis gas over corundum supported mixed oxides: one channel studies, Catal. Today 105 (2005) 367–371.
[19] V. Sadykov, S. Pavlova, Z. Vostrikov, N. Sazonova, E. Gubanova, R. Bunina, G. Alikina, A. Lukashevich, L. Pinaeva, L. Gogin, S. Pokrovskaya, V. Skomorokhov, A. Shigarov, C. Mirodatos, A. van Veen, A. Khristolyubov, V. Ulyanitskii, Performance of monolithic catalysts with complex active component in partial oxidation of methane into syngas: experimental studies and modeling, Stud. Surf. Sci. Catal. 167 (2007) 361–366.
[20] S. Pavlova, N. Sazonova, Yu. Ivanova, V. Sadykov, O. Snegurenko, V. Rogov, Partial oxidation of methane to synthesis gas over supported catalyst based on Pt-promoted mixed oxide, Catal. Today 91–92 (2004) 299.
[21] A. Cybulski, J.A. Moulijn, Monoliths in heterogeneous catalysis, Catal. Rev. Sci. Eng. 36 (1994) 179–270.
[22] G.F. Froment, K.B. Bischoff, Chemical Reactor Analysis and Design, Wiley, New York, 1979.
[23] E. Tronconi, P. Forzatti, Adequacy of lumped parameter models for SCR reactors with monolith structure, AIChE J. 38 (1992) 201–210.